Supporting Information

Mesoporous Gold Decorated MXene ($Ti_3C_2T_x$) Flexible Composite Films for Photo-Enhanced Solid-State Micro Supercapacitors

Yijia Luo,[1,2] Wenxiu Que,[1] Asep Sugih Nugraha,[3] Yunqing Kang,[2] Yi Tang,[4] Zhenwei Wu,[5] Joel Henzie*,[2] and Yusuke Yamauchi*[3,6,7]*

1. Electronic Materials Research Laboratory, Key Laboratory of the Ministry of Education & International Center for Dielectric Research, Shaanxi Engineering Research Center of Advanced Energy Materials and Devices, School of Electronic Science and Engineering, Xi'an Jiaotong University, No. 28, Xianning West Road, Xi'an, Shaanxi 710049, P. R. China
E-mail: wxque@mail.xjtu.edu.cn (Prof. W. Que)
2. Research Center for Materials Nanoarchitectonics (MANA), National Institute for Materials Science (NIMS), 1-1 Namiki, Tsukuba, Ibaraki 305-0044, Japan
E-mail: henzie.joeladam@nims.go.jp (Dr. J. Henzie)
3. Australian Institute for Bioengineering and Nanotechnology (AIBN), The University of Queensland, Brisbane QLD 4072, Australia
4. College of Materials Science and Engineering, Xi'an University of Science and Technology, Xi'an, Shaanxi 710054, P. R. China
5. Key Laboratory of Bio-based Material Science and Technology of the Ministry of Education, Northeast Forestry University, Harbin, Heilongjiang 150040, China
6. Department of Materials Process Engineering, Graduate School of Engineering, Nagoya University, Nagoya 464-8603, Japan
7. Department of Chemical and Biomolecular Engineering, Yonsei University, Seoul 03722, South Korea
E-mail: y.yamauchi@uq.edu.au (Prof. Y. Yamauchi)

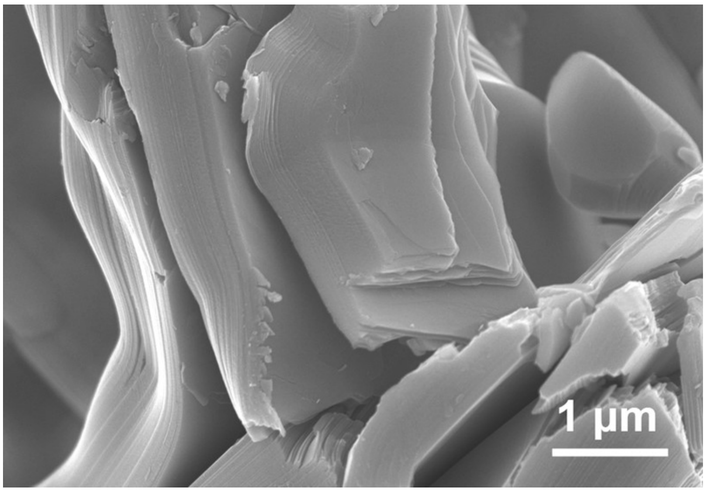

Figure S1 The SEM image of Ti_3AlC_2 powder.

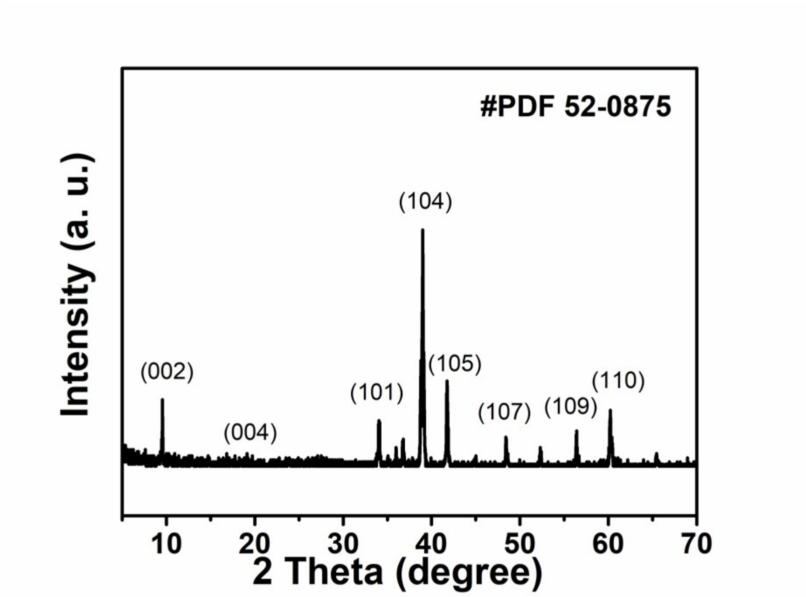

Figure S2 The XRD pattern of Ti_3AlC_2 powder.

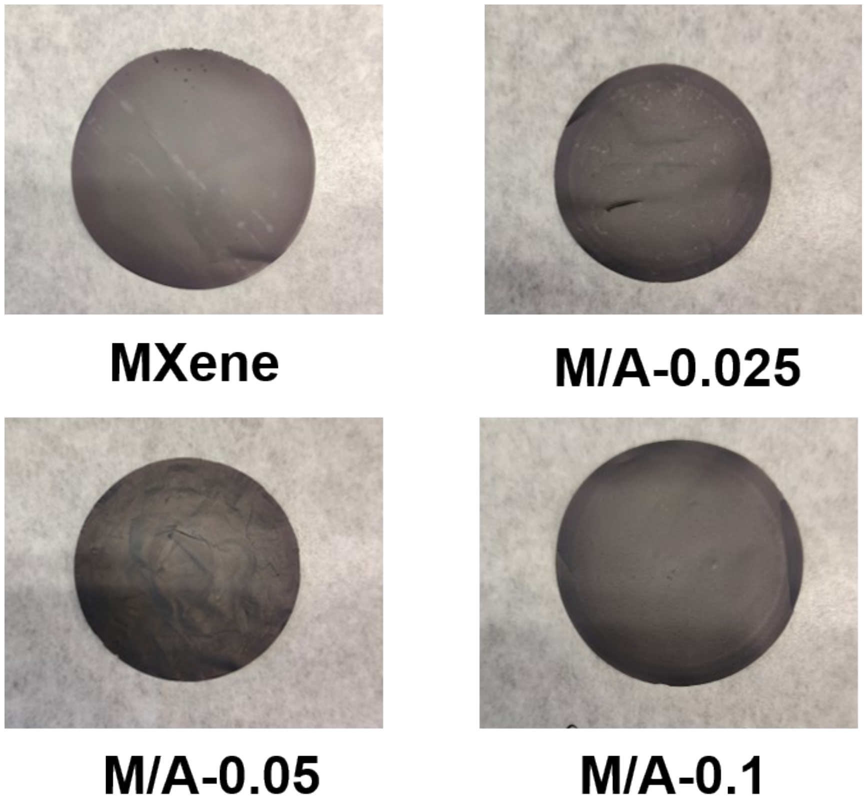

Figure S3 Top-view photographs of the prepared flexible films.

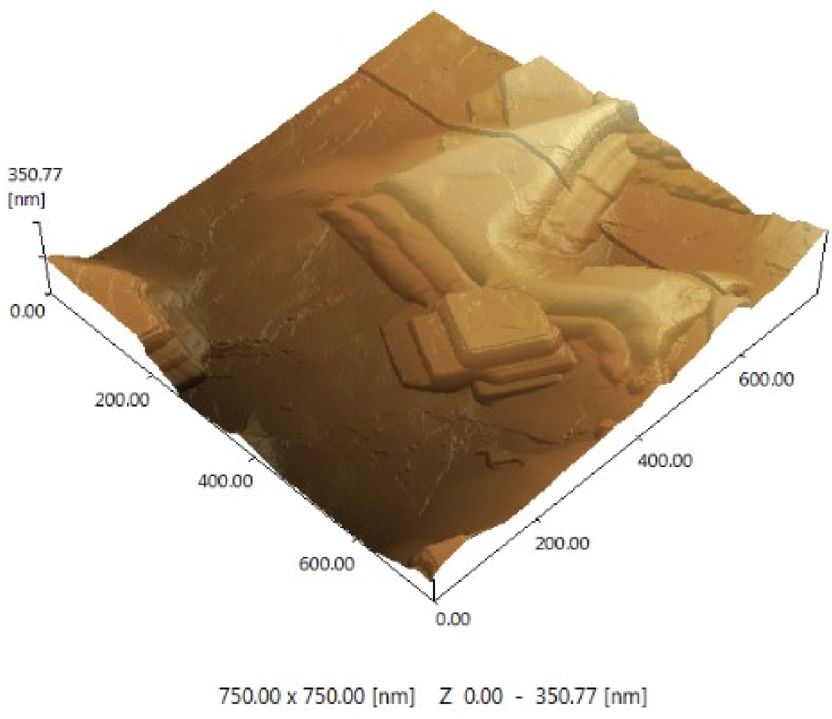

Figure S4 3D AFM image of the multilayer MXene flakes.

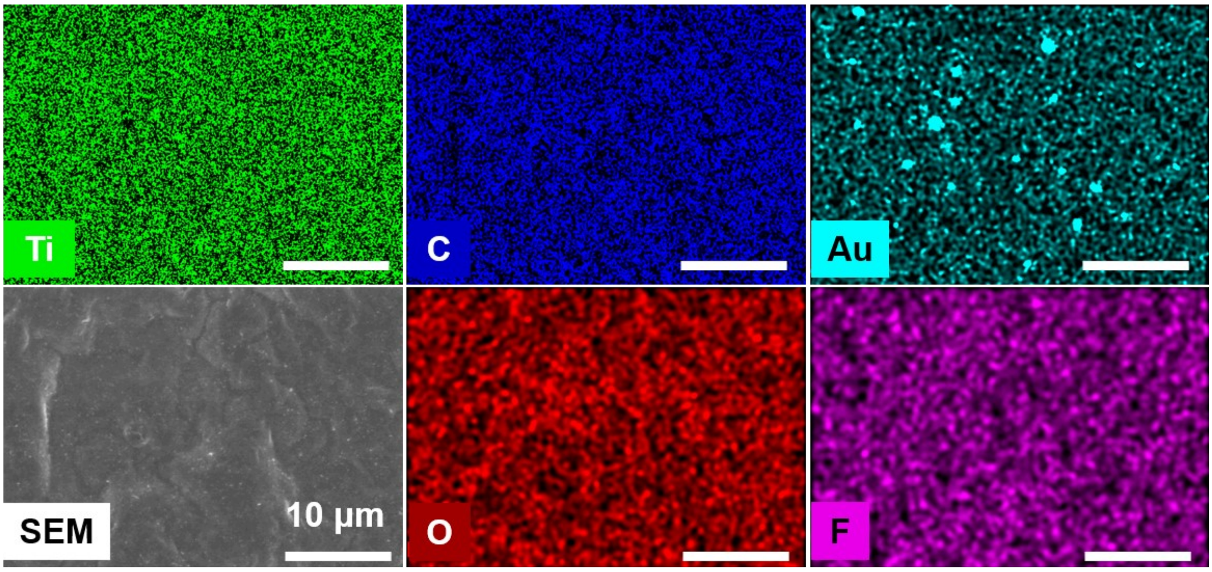

Figure S5 SEM-EDS elemental mapping images of M/A-0.05 flexible film (Surface).

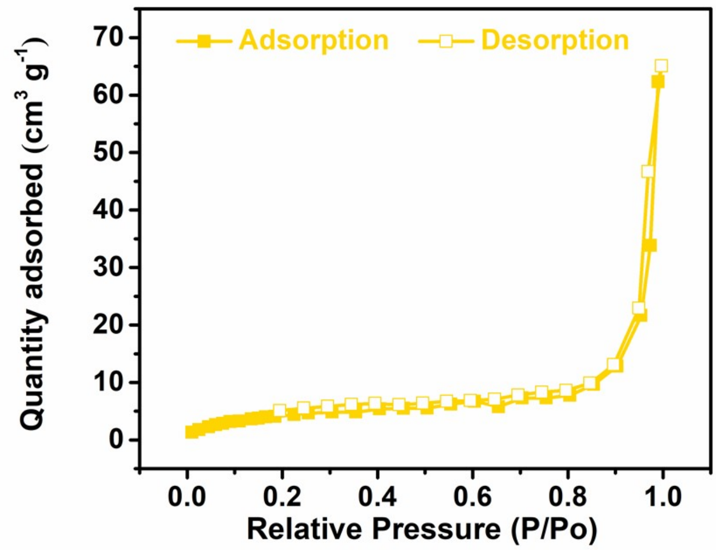

Figure S6 The N_2 adsorption/desorption analysis of the mesoporous Au NPs.

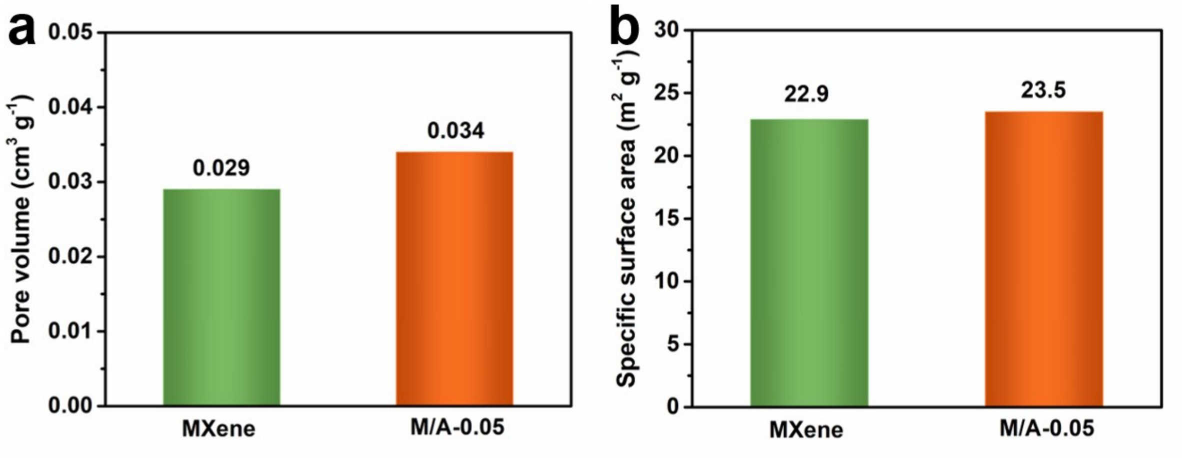

Figure S7 The N_2 adsorption/desorption analysis of the MXene and M/A-0.05 films. (a) pore volume. (b) specific surface area.

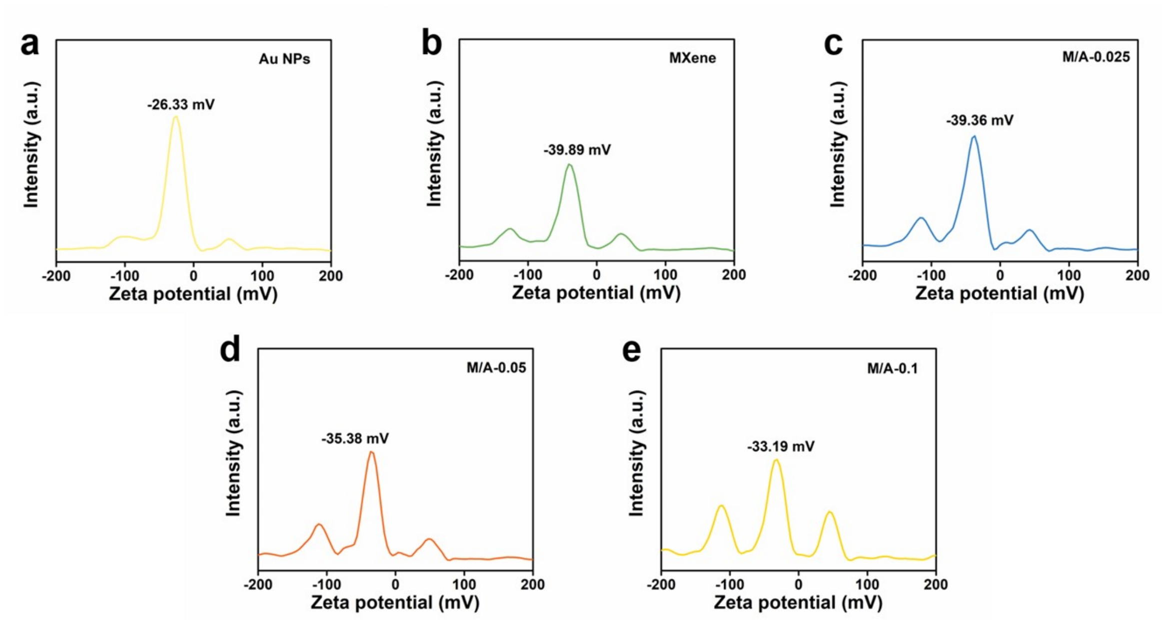

Figure S8 Mobility distribution of the (a) mesoporous Au NPs. (b) MXene. (c) M/A-0.025. (d) M/A-0.05. (e) M/A-0.1.

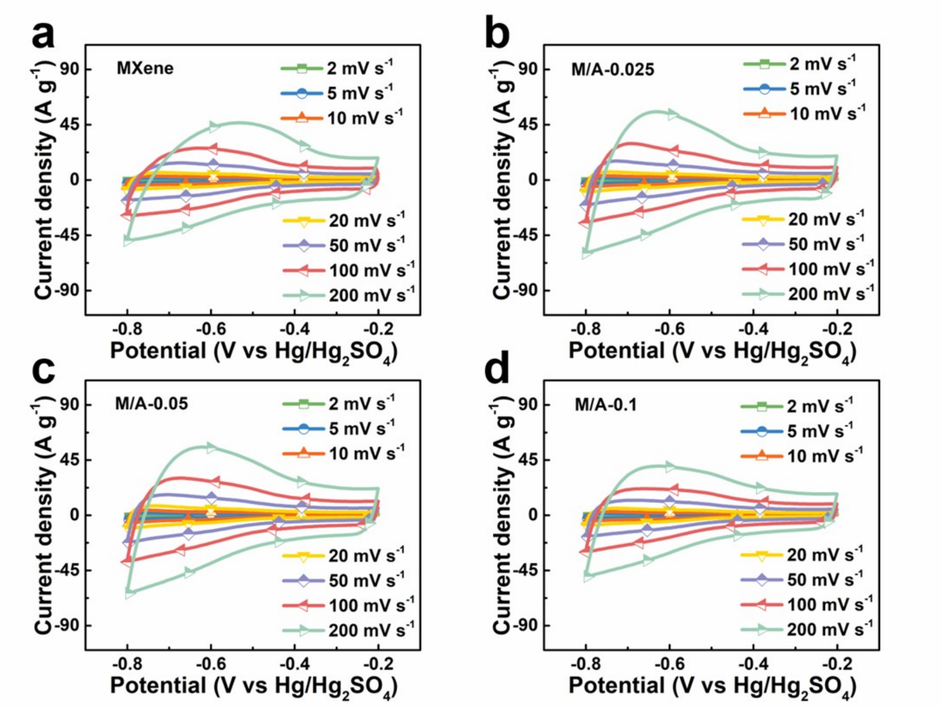

Figure S9 Electrochemical performance of the film electrodes by Swagelok three-electrode system in 3M H_2SO_4. CV curves of (a) MXene, (b) M/A-0.025, (c) M/A-0.1, and (d) M/A-0.1 at scan rates range from 2 to 200 mV s^{-1}.

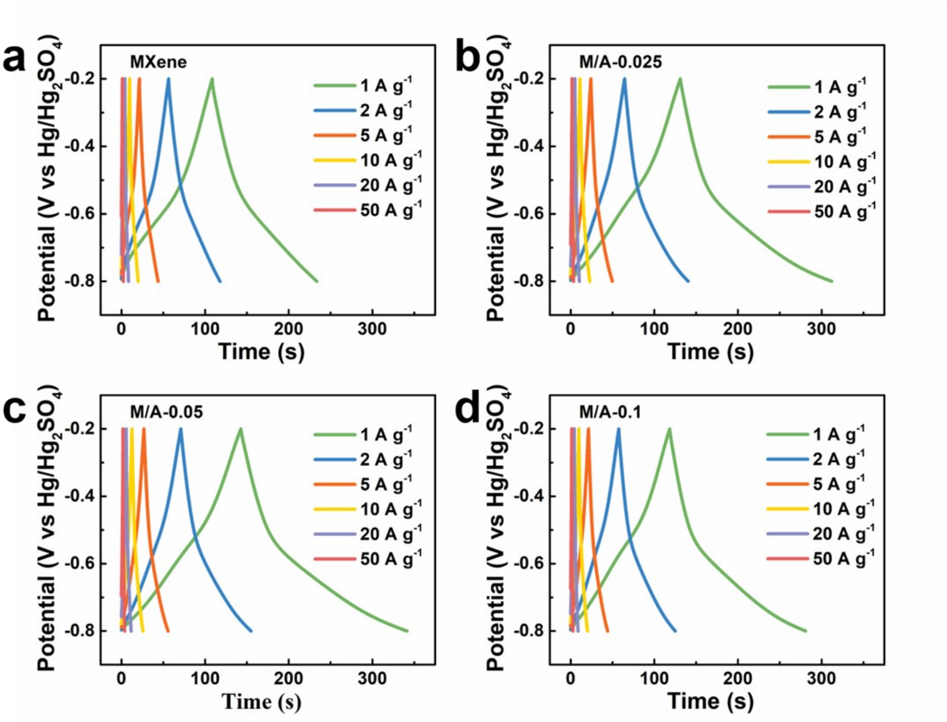

Figure S10 Electrochemical performance of the film electrodes by Swagelok three-electrode system in 3M H_2SO_4. GCD curves of (a) MXene, (b) M/A-0.025, (c) M/A-0.05, and (d) M/A-0.1 at current densities range from 1 to 50 A g^{-1}.

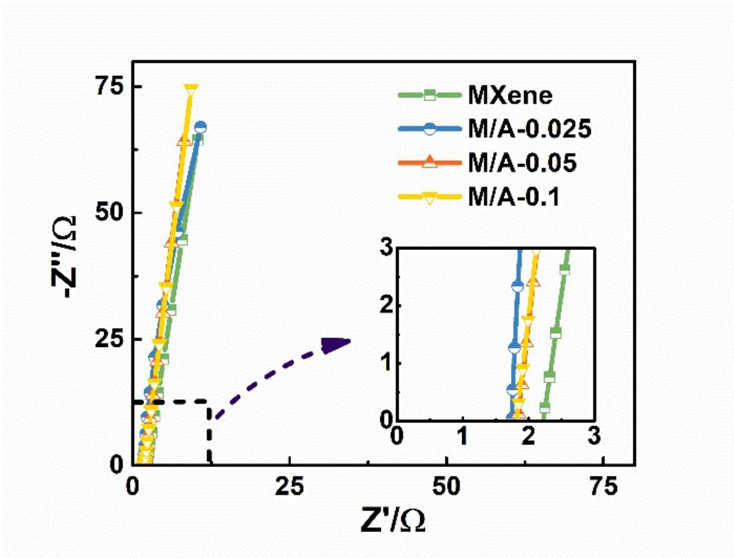

Figure S11 The fitted Nyquist plots of all film electrodes.

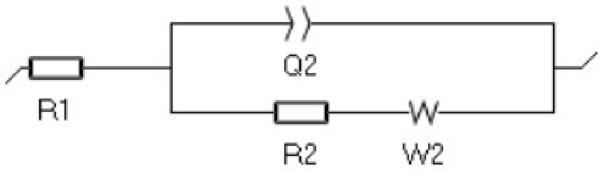

Figure S12 The equivalent circle model - Randles circuit.

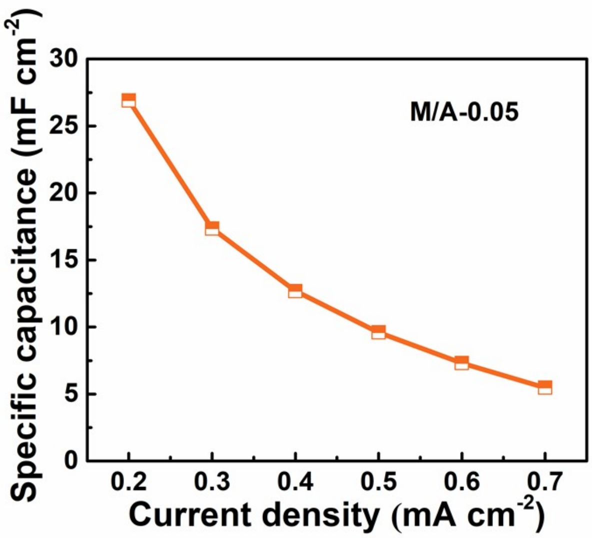

Figure S13 The areal specific capacitance of the M/A-0.05 film MSC device at different current densities.

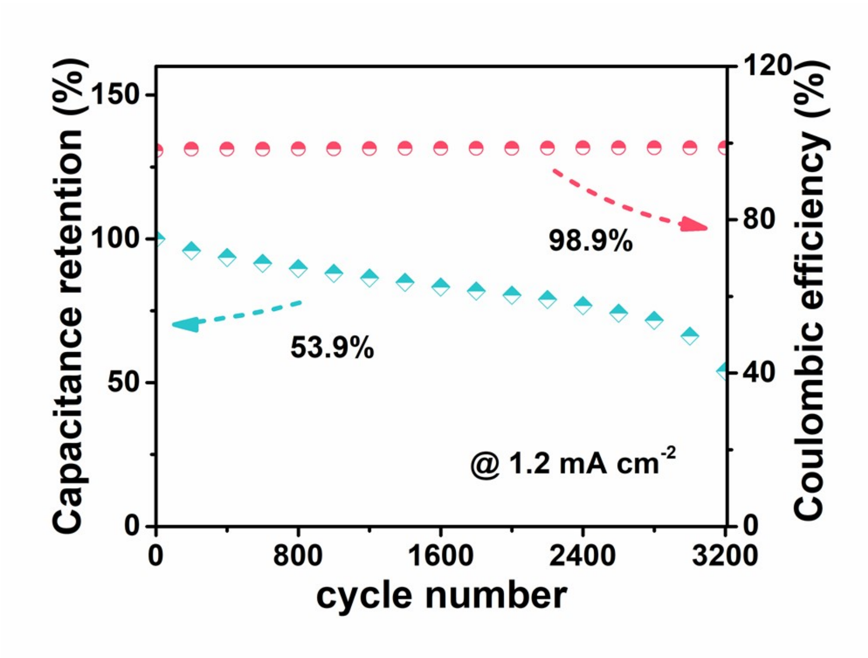

Figure S14 The capacitance retention and coulombic efficiency of the MXene film MSC devices.

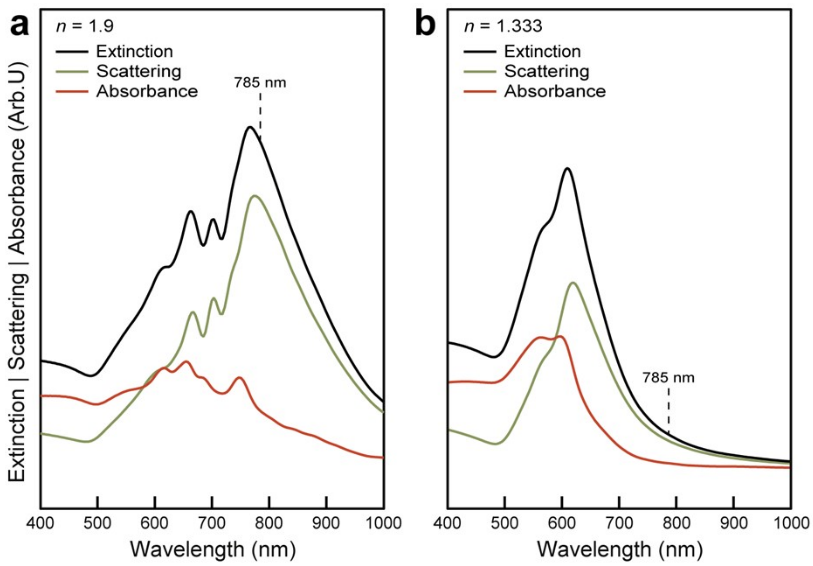

Figure S15 Extinction, scattering and absorbance cross sections of a 120 nm diameter mesoporous Au NP with 24 nm diameter pores suspended in a refractive index (*n*) of 1.9 (a) and 1.333 (b) to mimic MXene and water, respectively.

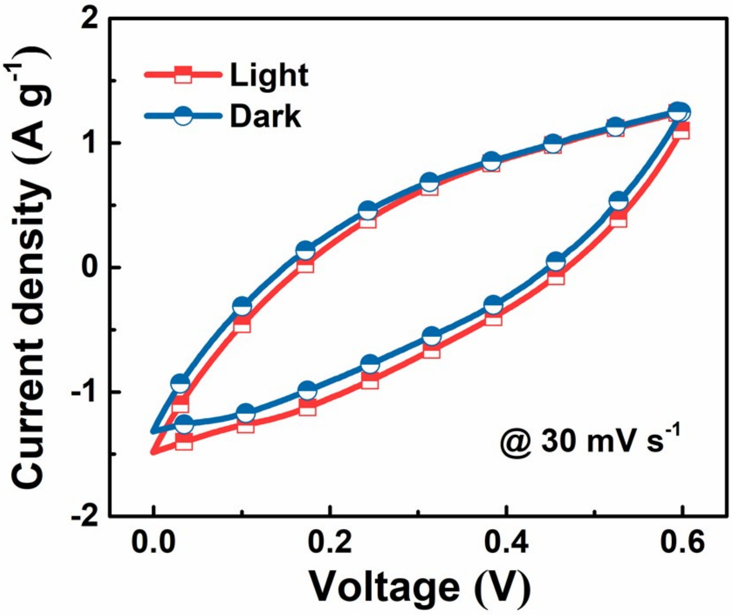

Figure S16 CV curves of the M/A-0.05 film MSC device in the presence and absence of light.

Table S1 Test results of Sheet Resistance value ($R_{\square}$), and the corresponding calculated resistivities (ρ) and conductivities (σ) of MXene and M/A-0.05 films.

Sample	$R_{\square}$ (Ω sq^{-1})	ρ (Ω cm)	σ (S cm^{-1})
MXene	0.7637	3.819×10^{-4}	2619
M/A-0.05	0.6886	3.443×10^{-4}	2904

Table S2 Dimensions of the symmetric MSC pattern.

Name	Size/mm
Interspace, I	2
Height, H	22
Width, W	4
Edge, E	2
Length, L	20